PCCP

Cite this: *Phys. Chem. Chem. Phys.*, 2011, **13**, 10690–10698

www.rsc.org/pccp

PAPER

Temperature dependence of the Fricke dosimeter and spur expansion time in the low-LET high-temperature radiolysis of water up to 350 °C: a Monte-Carlo simulation study

Sunuchakan Sanguanmith,[a] Yusa Muroya,[ab] Thititip Tippayamontri,[a] Jintana Meesungnoen,[a] Mingzhang Lin,[c] Yosuke Katsumura[b] and Jean-Paul Jay-Gerin*[a]

Received 3rd February 2011, Accepted 5th April 2011
DOI: 10.1039/c1cp20293f

Monte-Carlo simulations of the radiolysis of the ferrous sulfate (Fricke) dosimeter with low-linear energy transfer (LET) radiation (such as ^{60}Co γ-rays or fast electrons) have been performed as a function of temperature from 25 to 350 °C. The predicted yields of Fe^{2+} oxidation are found to increase with increasing temperature up to ~100–150 °C, and then tend to remain essentially constant at higher temperatures, in very good agreement with experiment. By using a simple method based on the direct application of the stoichiometric relationship that exists between the ferric ion yields so obtained $G(Fe^{3+})$ and the sum $\{3\,[g(e^-_{aq} + H^\bullet) + g(HO_2^\bullet)] + g(^\bullet OH) + 2\,g(H_2O_2)\}$, where $g(e^-_{aq} + H^\bullet)$, $g(HO_2^\bullet)$, $g(^\bullet OH)$, and $g(H_2O_2)$ are the primary radical and molecular yields of the radiolysis of deaerated 0.4 M H_2SO_4 aqueous solutions, the lifetime (τ_s) of the spur and its temperature dependence have been determined. In the spirit of the spur model, τ_s is an important indicator for overlapping spurs, giving the time required for the changeover from nonhomogeneous spur kinetics to homogeneous kinetics in the bulk solution. The calculations show that τ_s decreases by about an order of magnitude over the 25–350 °C temperature range, going from ~4.2×10^{-7} s at 25 °C to ~5.7×10^{-8} s at 350 °C. This decrease in τ_s with increasing temperature mainly originates from the quicker diffusion of the individual species involved. Moreover, the observed dependence of $G(Fe^{3+})$ on temperature largely reflects the influence of temperature upon the primary free-radical product yields of the radiolysis, especially the yield of $H^\bullet$ atoms. Above ~200–250 °C, the more and more pronounced intervention of the reaction of $H^\bullet$ atoms with water also contributes to the variation of $G(Fe^{3+})$, which may decrease or increase slightly, depending on the choice made for the rate constant of this reaction. All calculations reported herein use the radiolysis database of Elliot (Atomic Energy of Canada Limited) and Bartels (University of Notre Dame) that contains all the best currently available information on the rate constants, reaction mechanisms, and *g*-values in the range 20 to 350 °C.

I. Introduction

The radiation chemistry of liquid water is of considerable importance, not only for the intrinsic scientific interest it generates, but as well, because of its relevance to a number of practical applications. It is particularly important in radiation biology where living cells are composed of about 70–85% water by weight, and also in a number of domains of nuclear science and technology, such as in water-cooled nuclear power reactors where a quantitative understanding of the yields and activities of decomposition products of water is needed in order to mitigate the effects of water radiolysis and thus limit unwanted corrosion and degradation of materials by oxidizing species. A good summary of the present status of aqueous radiation chemistry is given in ref. 1–7.

The radiolysis of pure, deaerated liquid water by low-LET (linear energy transfer or energy loss per unit track length, $-dE/dx$), sparsely ionizing radiation (such as ^{60}Co γ-rays, fast electrons, or high-energy protons), at room temperature, is generally well understood. Briefly, it leads to the formation of

[a] *Département de Médecine Nucléaire et de Radiobiologie, Faculté de Médecine et des Sciences de la Santé, Université de Sherbrooke, 3001, 12ème Avenue Nord, Sherbrooke (Québec) J1H 5N4, Canada. E-mail: jean-paul.jay-gerin@USherbrooke.ca; Fax: +1 819-564-5442; Tel: +1 819-346-1110, ext. 14682/14773*
[b] *Nuclear Professional School, School of Engineering, University of Tokyo, 2-22 Shirakata-shirane, Tokai, Naka, Ibaraki 319-1188, Japan*
[c] *Nuclear Science and Engineering Directorate, Japan Atomic Energy Agency, 2-4 Shirakata-shirane, Tokai, Naka, Ibaraki 319-1195, Japan*

the free radicals and molecular products e^-_{aq} (the "hydrated" electron), OH^-, H_3O^+, $H^\bullet$, $^\bullet OH$, H_2, H_2O_2, $HO_2^\bullet/O_2^{\bullet-}$ (pK_a = 4.8 at 25 °C), *etc*. Under usual irradiation conditions (*i.e*., at modest dose rates), these species are generated non-homogeneously on subpicosecond time scales in small, spatially well-separated regions of dense ionization and excitation events, called "spurs",[8,9] along the track of the incident radiation. Owing to diffusion from their initial positions, the radiolytic products then either react within the spurs as they develop in time or escape into the bulk solution. The so-called "primary" radical and molecular yields (or "escape" yields) $g(e^-_{aq})$, $g(H^\bullet)$, $g(^\bullet OH)$, $g(H_2)$, $g(H_2O_2)$, *etc*., represent the numbers of species of each kind formed or destroyed per 100 eV of absorbed energy that remain after spur expansion.[10] At 25 °C, the lifetime of a spur is generally taken to be $\sim 10^{-7}$–10^{-6} s. By this time, the species that have escaped from spur reactions become homogeneously distributed throughout the bulk of the solution and available to react with dissolved solutes (if any) present (in moderate concentrations) at the time of irradiation.

At elevated temperatures, however, the time at which the homogeneous chemistry takes over within the solution is not well determined, even if one can expect the changeover from (nonhomogeneous) spur kinetics to homogeneous kinetics to occur faster than at ambient temperature. In fact, our earlier Monte-Carlo simulations already indicated that the time at which the nonhomogeneous chemical stage is completed diminishes with increasing temperature.[11,12] Such a trend was also observed in recent measurements of the fast spur decay kinetics of e^-_{aq} using pulse radiolysis in the picosecond/nanosecond time range at elevated temperatures.[13,14] The present study is precisely an attempt to quantitatively assess the temperature dependence of the spur expansion, more specifically the "spur expansion" time or yet the duration of nonhomogeneity (nonhomogeneous to homogeneous conversion time)—called τ_s thereafter—from ambient up to 350 °C. The approach adopted here employs Monte-Carlo simulations of the radiolysis of the ferrous sulfate (Fricke) dosimeter,[15] as described below.

II. The Fricke dosimeter

One of the most studied systems in radiation chemistry is the air-saturated ($\sim 2.5 \times 10^{-4}$ M O_2) solution of 1–10 mM ferrous sulfate in aqueous 0.4 M H_2SO_4, which is referred to as the "Fricke dosimeter" after Hugo Fricke, who first published accounts of its properties in 1927–1929.[16] Of all aqueous systems studied, the Fricke dosimeter is certainly the best understood, and the most widely used, liquid chemical dosimeter. Much has already been published on its underlying reaction mechanism and response in a wide variety of scenarios including LET and temperature effects.[15,17] The chemistry of this system is based upon the oxidation of ferrous ions to ferric ions by the species $H^\bullet$, $HO_2^\bullet$, $^\bullet OH$, and H_2O_2[18] that are formed in the water of the irradiated solution under aerated conditions.[1,15,19–21] From this mechanism, the yield of Fe^{3+} ions in an irradiated Fricke dosimeter can readily be expressed in terms of the escape yields (*i.e*., at τ_s) of the radical and molecular products of the radiolysis of air-free 0.4 M H_2SO_4 aqueous solution by the following stoichiometric equation:[1,19,21]

$$G(Fe^{3+}) = 3[g(e^-_{aq} + H^\bullet) + g(HO_2^\bullet)] + g(^\bullet OH) + 2g(H_2O_2), \quad (1)$$

where $g(e^-_{aq} + H^\bullet)$ represents the sum of the primary yields of the reducing radicals e^-_{aq} and $H^\bullet$.

III. Procedure used to estimate the "spur expansion" time τ_s

A simple procedure, based on the use of eqn (1) (*i.e*., on the well-established reaction mechanism of the Fricke dosimeter), has been implemented to determine τ_s and its dependence on temperature from ambient up to 350 °C. This procedure involves the following *three* steps: (i) a direct Monte-Carlo simulation of the radiolytic oxidation of Fe^{2+} to Fe^{3+} in the aerated Fricke dosimeter is first conducted in order to determine $G(Fe^{3+})$ as a function of temperature; (ii) Monte-Carlo simulations of the radiolysis of air-free 0.4 M H_2SO_4 aqueous solutions are next performed to determine, for the 25–350 °C temperature range studied, the yields of the species $H^\bullet$, $HO_2^\bullet$, $^\bullet OH$, and H_2O_2 that are involved in eqn (1) as a function of time during the nonhomogeneous chemical stage (*i.e*., during spur expansion);[22] and (iii) the lifetime of the spur τ_s and its temperature dependence are then readily obtained by identifying, at each considered temperature, the coordinates of the intersection of the curve showing the *directly* simulated ferric ion yields and the corresponding yield values *calculated* using eqn (1) *at different selected times*. These various steps are described in more detail below.

IV. Monte-Carlo simulations

Monte-Carlo simulation methods are used to model the complex sequence of events that are generated in liquid water following absorption of ionization radiation. Such a procedure is particularly well-suited to account for the stochastic nature of the phenomena. The detailed description and implementation of our Monte-Carlo code IONLYS-IRT that simulates the radiolysis of air-free aqueous 0.4 M H_2SO_4 solutions (pH $\approx$ 0.46) and the radiation-induced oxidation of ferrous sulfate solutions in the (aerated) Fricke dosimeter at both ambient and elevated temperatures have been given previously.[7,11,21,23] In brief, the IONLYS simulation program covers the early "physical" and "physicochemical" stages of radiation action up to $\sim 10^{-12}$ s. It models, event by event, all the basic physical interactions (energy deposition) and the subsequent establishment of thermal equilibrium in the system (conversion of the physical products created locally after completion of the physical stage into the various initial radical and molecular products of the radiolysis, distributed in a highly nonhomogeneous track structure). The complex spatial distribution of reactants at the end of the physicochemical stage, which is provided as an output of the IONLYS program, is then used directly as the starting point for the subsequent "nonhomogeneous chemical" stage (from $\sim 10^{-12}$ to $\sim 10^{-7}$–10^{-6} s at 25 °C). This third stage, during which the individual reactive species diffuse randomly at rates

determined by their diffusion coefficients and react with one another or, competitively, with any added solutes present at the time of irradiation (and for which the relevant reaction rates are known) until all spur processes are complete (at τ_s), is covered by our IRT program. This IRT program can obviously also be used efficiently to describe the "homogeneous" chemical stage that takes place at longer times, as is the case here for the simulation of the Fricke dosimeter in which ferric ions are produced at a wide variety of times. This program employs the "independent reaction times" (IRT) method, a computer efficient stochastic simulation technique that is used to simulate reaction times without following the trajectories of the diffusing species.[24,25] Its implementation has been described in detail.[26] The ability of this program to give accurate time-dependent chemical yields under different irradiation conditions has been well validated by comparison with full random flights (or "step-by-step") Monte-Carlo simulations, which do follow the reactant trajectories in detail.[27,28]

The effects of the background concentration of H^+ in aqueous 0.4 M sulfuric acid solutions were added to the IRT program as pseudo first-order reactions. We also supplemented the reaction scheme for the radiolysis of pure deaerated liquid water[6,7,26,29] to include the reactions that account for the species (HSO_4^-, SO_4^{2-}, $SO_4^{\bullet -}$, and $S_2O_8^{2-}$) present in irradiated aqueous H_2SO_4 solutions.[7,21,30] In addition, we introduced the effect of ionic strength of the solutions on all reactions between ions.[7,21,31] Over the 25–350 °C temperature range studied, the correction to the reaction rate constants was made using the following equation[32,33]

$$\log\left(\frac{k}{k_0}\right) = 3.64 \times 10^6 \frac{Z_a Z_b}{(\varepsilon T)^{3/2}} \left(\frac{I^{1/2}}{1 + I^{1/2}}\right) \qquad (2)$$

where k is the rate constant at ionic strength I, k_0 is the rate constant in the limit of zero ionic strength (*i.e.*, at infinite dilution of ions), Z_a and Z_b are the algebraic numbers of charges on the reactants (positive for cations and negative for anions), T is the absolute temperature (in K), ε is the dielectric constant of the medium (for water, ε = 78.5 at 25 °C and 13.0 at 350 °C), and I (in M) is defined as:[34]

$$I = \frac{1}{2}\sum_i Z_i^2 C_i \qquad (3)$$

where Z_i is the charge number of the i_{th} ion and C_i is its molar concentration (the sum extends over all ionic species present in the solution). According to eqn (2), the rate constants will increase, decrease, or remain the same with increasing ionic strength, depending on whether the ions have the same sign, opposite signs, or whether one species is uncharged. Finally, in our simulations the "direct" action of ionizing radiation on the sulfuric acid anions (mainly the hydrogen sulfate ion HSO_4^-) was neglected, which is a reasonably good approximation in the sulfuric acid concentration studied.[35]

To stochastically model the chemistry of the Fricke dosimeter, we added to the IRT program the reactions of Fe^{2+} ions with the oxidizing species $HO_2^{\bullet}$, $^{\bullet}OH$, and H_2O_2 that are formed in the water of the irradiated solutions under aerated conditions.[7,21,36] Under normal irradiation conditions, the radical concentrations are low compared with the background concentrations of Fe^{2+} ions and O_2 in solution, and those reactions were treated in the IRT program as pseudo first-order. The values of the rate constants at 25 °C of the individual reactions taking place in the radiolytic oxidation of Fe^{2+} ions to Fe^{3+} have previously been determined.[7,21,29,37–39] The most rapid reaction of Fe^{2+} ions is with $^{\bullet}OH$ radicals ($k = 3.4 \times 10^8$ M^{-1} s^{-1}) while the slowest component of the kinetics of Fe^{3+} formation is due to the reaction of Fe^{2+} with hydrogen peroxide (k = 52 M^{-1} s^{-1}). For example, in the case of 5 mM $FeSO_4$ solutions considered in this work, the (Fenton-type) reaction[40]

$$Fe^{2+} + H_2O_2 \rightarrow Fe^{3+} + {}^{\bullet}OH + OH^- \qquad (4)$$

takes several seconds to go to completion,[21] which significantly increases the computer time usually needed for modeling the radiolysis of liquid water. The remaining intermediate stage is due to the reaction of Fe^{2+} with hydroperoxyl radicals ($k = 7.9 \times 10^5$ M^{-1} s^{-1}). In the simulations reported here, the time evolution of $G(Fe^{3+})$ was followed until ~50–200 s.

As for the calculations of $G(Fe^{3+})$ as a function of temperature from ambient up to 350 °C, we used an extended version of our IONLYS-IRT code which was developed previously to include the effects of high temperature on the low-LET radiolysis of liquid water.[7,11,41] The important parameters are the yields of the primary products of water radiolysis and the rate constants of their inter-reactions. In this version of IONLYS-IRT, we used the radiolysis database, including rate constants, diffusion coefficients, reaction mechanisms, and g-values, recently compiled by Elliot and Bartels.[6] This new database provides a recommendation for the *best* values to use in high-temperature modeling of water radiolysis up to 350 °C. In addition, the inclusion in the simulations of the rapid drop observed in the rate of the self-reaction of e^-_{aq} above 150 °C[6,42] (contrary to previous work) led us to re-evaluate the temperature dependence of some parameters involved in the early physicochemical stage of the radiolysis, namely, the electron thermalization distance (r_{th}), the dissociative electron attachment (DEA), and the branching ratios of the different excited water molecule decomposition channels. The details of this re-evaluation are published elsewhere[41] but we briefly summarize them here. In essence, the values of r_{th} were obtained from comparing our simulated time-dependent e^-_{aq} yield data to recent picosecond (~60 ps to 6 ns) and conventional nanosecond (using e^-_{aq} scavenging by methyl viologen MV^{2+}) pulse radiolysis measurements of the decay kinetics of e^-_{aq} at several different temperatures between 25 and 350 °C.[14] Using this best fitting procedure, r_{th}—defined as the length of the vector ($|\boldsymbol{R}_f - \boldsymbol{R}_i|$) from the point of departure ($\boldsymbol{R}_i$) to the final ($\boldsymbol{R}_f$) position of the electron after thermalization—was found to remain essentially unchanged up to ~100–150 °C (and equal to its value at 25 °C), but to decrease sharply at higher temperatures with $r_{th}/r_{th}(25\ °C) \approx 0.29$ at 350 °C.[41] Physically, this decrease in r_{th} above 100–150 °C was interpreted as indicating an increase in the scattering cross-sections of subexcitation electrons (e^-_{sub})[43] that accounts for a loss of structural order of water molecules due to an increasing breaking of hydrogen bonds with temperature.[44] Building on these findings on r_{th}, we also

incorporated in our modeling calculations a dependence on temperature of the dissociative attachment of subexcitation electrons and of the branching ratios of the different decay channels for excited water molecules (as r_{th}, these other physicochemical parameters are sensitive to the local structural order of water). This dependence was in a functional form *similar* to that of r_{th}, *i.e.*, taken constant up to ~100–150 °C and then followed by a marked discontinuity around these temperatures. In the absence of other detailed experimental information, the values of these latter parameters at 350 °C were assumed to be equal to those observed in water *vapor*,[41] a procedure that has already been used previously.[45]

The temperature dependences of the rate constants for the ferrous ion reactions with •OH, HO_2•, and H_2O_2 were scaled from their values at 25 °C using simple Arrhenius equations with activation energies of 9.2, 42, and 42 kJ mol^{-1}, respectively.[37–40,46,47] Finally, as there are no experimental data available on the temperature dependences of the diffusion coefficients of the Fe^{2+} and Fe^{3+} ions, the procedure adopted here was to scale the 25 °C values (0.719×10^{-9} and 0.604×10^{-9} m^2 s^{-1}, respectively)[48] according to the self-diffusion in liquid water.[11]

All Monte-Carlo simulations reported here were performed along the liquid-vapor coexistence curve, the density of the pressurized water decreasing from 1 g cm^{-3} (1 bar or 0.1 MPa) at 25 °C to 0.575 g cm^{-3} (16.5 MPa) at 350 °C.[49] For this temperature range, calculations show that *g*-values vary only little with the applied pressure (density). Finally, to reproduce the effects of fast electron or ^{60}Co γ-ray radiolysis, we used short (typically, ~150 μm) segments of 300 MeV proton tracks, over which the average LET value obtained in the simulations was nearly constant and equal to ~0.3 keV μm^{-1} at 25 °C.[50] Such model calculations thus gave "track segment" yields at a well-defined LET.[4] The number of proton histories (usually ~150) was chosen so as to ensure only small statistical fluctuations in the computed averages of chemical yields, while keeping acceptable computer time limits.

V. Results and discussion

Fig. 1 shows the time evolution of $G(Fe^{3+})$ as obtained from our simulations of the radiolysis of the Fricke dosimeter by 300 MeV incident protons at different temperatures in the range 25–350 °C. As we can see from this figure, $G(Fe^{3+})$ is time dependent as a result of the differences in the lifetimes of the reactions occurring in the oxidation of ferrous sulfate by radiation.[1,15,19,21,38,39] All reactions take place faster at higher temperature. The kinetics of Fe^{3+} formation at 350 °C is several orders of magnitude faster than at room temperature. Also, an interesting feature shown in this figure is the increase of $G(Fe^{3+})$ with temperature up to ~100–150 °C, followed by stabilization to a value essentially constant at higher temperatures. The influence of the irradiation temperature on the Fricke yield is further illustrated in Fig. 2 over the range 25–350 °C. As can be seen, a very good agreement is obtained between our computed Fe^{3+} yields and the available experimental data.[44,51–54] Interestingly, the predicted yield of Fe^{3+} increases from ~15.4 to 16.7 molec./100 eV on going from 25 to 150 °C, which corresponds to a temperature coefficient of ~1.0% per degree over this range of temperature.[55]

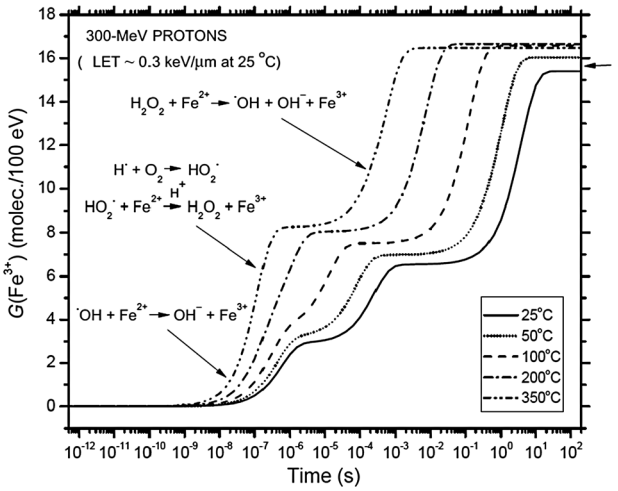

Fig. 1 Time evolution of $G(Fe^{3+})$ (in molec./100 eV) for 300 MeV incident protons (LET ≈ 0.3 keV μm^{-1} at 25 °C) in air-saturated solutions of 5 mM $FeSO_4$ in aqueous 0.4 M H_2SO_4 at different temperatures in the range 25–350 °C. The different lines correspond to our theoretical simulations at 25 °C (solid line), 50 °C (dotted line), 100 °C (dashed line), 200 °C (dash-dot line), and 350 °C (dash-dot-dot line) (see text). The arrow on the right of the figure shows the accepted value (15.6 molec./100 eV) of the yield of the Fricke dosimeter for ^{60}Co γ-rays and fast electrons at room temperature (see, for example, ref. 1, 15, 19, 21, and 50).

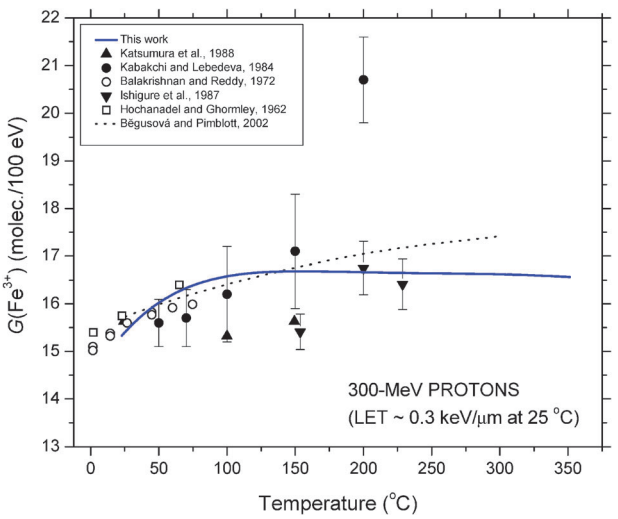

Fig. 2 Yield of Fe^{3+} ions (at ~50 s) (in molec./100 eV) in aerated Fricke (5 mM $FeSO_4$ in aqueous 0.4 M H_2SO_4) solutions as a function of temperature, for 300 MeV irradiating protons (LET ≈ 0.3 keV μm^{-1} at 25 °C). The solid line shows the values of $G(Fe^{3+})$ obtained from our Monte-Carlo simulations in the range 25–350 °C (see text). The dotted line represents the *G*-values for the Fricke dosimeter predicted by Běgusová and Pimblott (ref. 38) from stochastic IRT simulations employing simulated electron track structures. Experiment: (□) ref. 44, (▲) ref. 51, (●) ref. 52, (○) ref. 53, and (▼) ref. 54.

In Fig. 3, we show the *sensitivity* of our simulated Fricke yield results on variations in the value of the rate constant for the oxidation of water by the hydrogen atom:

$$H^{\bullet} + H_2O \rightarrow H_2 + {}^{\bullet}OH, \qquad (5)$$

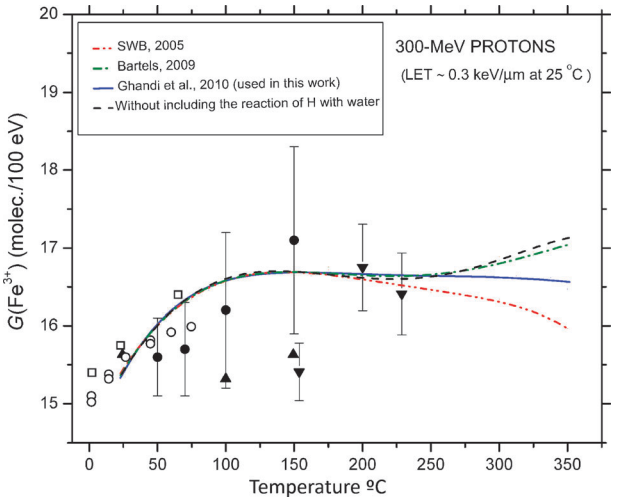

Fig. 3 Sensitivity of our Monte-Carlo simulations of the low-LET radiolysis of aerated Fricke (5 mM $FeSO_4$ in aqueous 0.4 M H_2SO_4) solutions to the value of the rate constant for the reaction of $H^{\bullet}$ atom with water. Simulated Fe^{3+} ion yields (in molec./100 eV) are obtained at ~50 s following ionization, over the studied range 25–350 °C (see text). Symbols, representing experimental data, are the same as in Fig. 2. The solid line (which is the same as that shown in Fig. 2) shows our computed results of $G(Fe^{3+})$ obtained with the reaction rate of 10^4 M^{-1} s^{-1} at 300 °C recently estimated by Ghandi and coworkers (ref. 59). Note that this rate was shown to best account for the observed H_2 formation above ~200–250 °C (ref. 41). The dash-dot line represents our $G(Fe^{3+})$ values computed with the rate constant proposed by Bartels (ref. 6 and 57) (2.2×10^3 M^{-1} s^{-1} at 300 °C), while the dash-dot-dot line shows our simulated results of $G(Fe^{3+})$ obtained with the rate constant suggested by Swiatla-Wojcik and Buxton (ref. 56) (3.2×10^4 M^{-1} s^{-1} at 300 °C). Finally, the dashed line represents our simulated results of $G(Fe^{3+})$ calculated without incorporating reaction (5) in the simulations.

which was recently suggested by Swiatla-Wojcik and Buxton (hereafter referred to as SWB)[56] to quantitatively explain the anomalous increase of the primary yield of H_2 in the low-LET radiolysis of water above ~200–250 °C.[6] Using deterministic diffusion-kinetic calculations, SWB inferred that a reaction rate constant of $\sim 3.2 \times 10^4$ M^{-1} s^{-1} was required to account for the observed additional yield of H_2 at 300 °C. This rate constant value, however, was disputed by Bartels[57] on the basis of thermodynamic arguments. This latter argued that reaction (5) could not be as fast as suggested and proposed that a better estimate of this number was rather $\sim 2.2 \times 10^3$ M^{-1} s^{-1} at 300 °C. In reply to these comments, Swiatla-Wojcik and Buxton[58] re-analyzed Bartels's thermodynamic estimate to eventually lead to a revised value of 1.75×10^4 M^{-1} s^{-1} for the rate constant at 300 °C. According to our own most recent Monte-Carlo simulations of the radiolysis of water at high temperatures,[41] it appears that reaction (5) is actually needed if we want to reproduce the unexplained increase in the H_2 yield above ~200 °C. Moreover, calculations[41] also show that a good agreement between simulated and experimental $g(H_2)$ results is obtained with the rate constant of $\sim 10^4$ M^{-1} s^{-1} at 300 °C, a value recently inferred by Ghandi and coworkers[59] from muon spin resonance spectroscopy experiments and also very close to that re-estimated by SWB.[58] Thus, all computations presented in this study were carried out by incorporating reaction (5) and using, unless otherwise specified, Ghandi *et al.*'s reported rate constant value. As we can see from Fig. 3, using SWB's rate constant[56] for reaction (5) leads to values of $G(Fe^{3+})$ that decrease slightly above ~200–250 °C. On the contrary, if we adopt the rate constant given by Bartels, the $G(Fe^{3+})$ values so obtained increase slightly at elevated temperatures. The choice of Ghandi *et al.*'s rate constant for reaction (5), in turn, leads to values of $G(Fe^{3+})$ which are essentially insensitive to temperatures above ~150 °C. For the sake of reference, we also calculated $G(Fe^{3+})$ in complete absence of reaction (5). The results, shown in Fig. 3, indicate an increase in $G(Fe^{3+})$ above ~200–250 °C which is slightly higher than that found when using the reaction rate constant value proposed by Bartels. Unfortunately, there are no experimental data currently available in the literature in this range of temperatures with which to compare the above results. It thus appears difficult at present to conclude on the basis of this study only, on the importance of the role of reaction (5) in the low-LET radiolysis of water at high temperatures or, equivalently, on the rate constant that is indeed associated with this reaction.

As mentioned above, a simple three-step procedure, based on the use of eqn (1) of the Fricke dosimeter, was employed to determine the "spur expansion" time τ_s as a function of temperature from 25 to 350 °C. This procedure, illustrated in Fig. 4, can be described as follows (see also Section III).

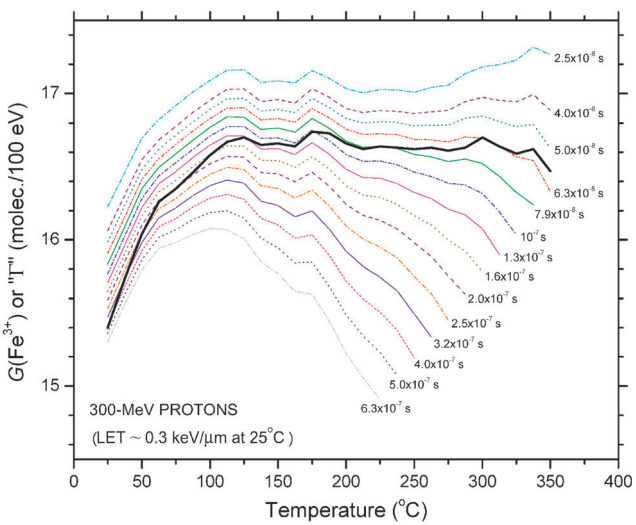

Fig. 4 Yield of Fe^{3+} ions (in molec./100 eV) in aerated Fricke (5 mM $FeSO_4$ in aqueous 0.4 M H_2SO_4) solutions as a function of temperature, for 300 MeV incident protons. The thick solid line shows the (raw) values of $G(Fe^{3+})$ obtained *directly* (at ~50 s) from our Monte-Carlo simulations (it is the same as the solid line shown in Fig. 2 and 3 after smoothing of the data). All the other curves (in different colors) show the "I" values calculated at different times between $\sim 10^{-6}$ and 10^{-8} s from the right-hand side of eqn (1) using the radical and molecular product yields obtained at each selected time from our Monte-Carlo simulations of the radiolysis of deaerated 0.4 M H_2SO_4 aqueous solutions. The time τ_s at which spur reactions are complete and its temperature dependence are obtained by simply identifying the coordinates of the intersections of the thick solid curve with all the other, time-parameterized curves (see text).

(i) Monte-Carlo simulations of the radiolytic oxidation of Fe^{2+} to Fe^{3+} in the aerated Fricke dosimeter irradiated by 300 MeV incident protons are first performed in order to directly determine $G(Fe^{3+})$ as a function of temperature. These $G(Fe^{3+})$ calculations, already presented in Fig. 1–3, are shown as the thick solid line in Fig. 4. Note that, in this figure, the computed values of $G(Fe^{3+})$ are shown in their raw form, unlike in Fig. 1–3 where these data have been smoothed.

(ii) Monte-Carlo simulations of the radiolysis of deaerated 0.4 M H_2SO_4 aqueous solutions (pH $\approx$ 0.46) are next carried out in the same irradiation conditions to determine, for temperatures in the range 25–350 °C, the yields of the species ($H^\bullet$, $HO_2^\bullet$, $^\bullet OH$, and H_2O_2) that are involved in eqn (1) at different selected times during the period of nonhomogeneous chemistry following irradiation (*i.e.*, during spur expansion). Using these yield values, the right-hand side of eqn (1)—which is of course not equal in general to the Fricke yield $G(Fe^{3+})$ and which we will thus call here "I" for the sake of convenience[22]—can then be calculated at each selected time between $\sim 10^{-8}$ and 10^{-6} s as a function of temperature. The various calculated curves of "I" *vs.* temperature, parameterized by time, thus obtained are shown in Fig. 4.

(iii) Finally, for the range of temperature studied, the times τ_s at which spur reactions are complete are obtained from the data displayed in Fig. 4 by simply identifying the intersections of the $G(Fe^{3+})$ *vs.* temperature curve *directly* obtained from the simulations in (i) with each of the "I" curves *vs.* temperature calculated from the right-hand side of eqn (1) at different times in (ii). The lifetime of the spur and its temperature dependence are then simply obtained from the coordinates of all those intersections (at these particular points, $G(Fe^{3+}) = "I"$). The corresponding values of τ_s are shown in Fig. 5 as a function of temperature.

The above procedure is particularly useful because it offers, to our knowledge for the first time, a quantitative estimate of the time required to observe the transition from nonhomogeneity to homogeneity in the distribution of the reactive species[60] formed in ^{60}Co-γ-irradiated water as the temperature is raised from 25 up to 350 °C. In the spirit of the spur model,[8,9] τ_s is an important indicator for overlapping spurs and the establishment of homogeneity following irradiation. In this regard, τ_s is well-known to be dependent on factors such as the quality of the radiation (LET) and the rate of energy deposition (*i.e.*, the dose rate). Here, we demonstrate that τ_s also strongly depends upon the irradiation temperature. Indeed, as can be seen from Fig. 5, τ_s is found to decrease over the temperature range studied by about an order of magnitude, from $\sim 4.2 \times 10^{-7}$ s at 25 °C to $\sim 5.7 \times 10^{-8}$ s at 350 °C.[61] This decrease in τ_s with increasing temperature, which essentially originates from the quicker diffusion of the individual species involved in spur reactions, was already identified in our earlier Monte-Carlo simulations of the radiolysis of water at high temperatures.[11,12] Experimentally, such a trend was also clearly observed recently, especially in the e^-_{aq} decay measurements of Baldacchino *et al.*[13] using pulse radiolysis in the picosecond/nanosecond time range from room temperature up to 350 °C. These authors observed that with increasing temperature the decay of e^-_{aq} became less and less pronounced. At 350 °C, they reported an almost flat signal

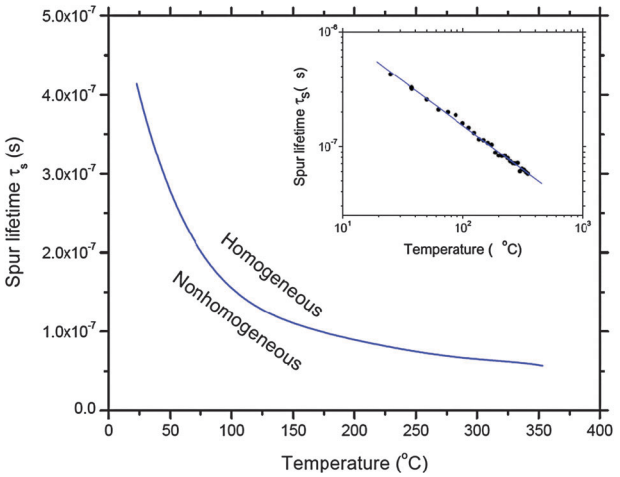

Fig. 5 Time of spur expansion τ_s as a function of temperature for low-LET irradiations of water. The solid line indicates the time required to observe, at a given temperature, the transition from nonhomogeneity to homogeneity in the distribution of the reactive species. τ_s markedly diminishes with increasing temperature, approaching a value of $\sim 5.7 \times 10^{-8}$ s at 350 °C. The inset shows a log–log plot of τ_s against temperature, the solid circles representing the coordinates of the intersections of the curve showing the *directly* simulated Fricke yields and those representing the "I" yields calculated from the right-hand side of eqn (1) at different times (see Fig. 4). The straight line was obtained from a least-squares fit of eqn (6) to the data (see text).

from $\sim$100 ps to 2.75 ns, suggesting an efficient escape of hydrated electrons from spur reactions. Similar conclusions were obtained by Muroya *et al.*,[14] who first reported the kinetics of the decay of e^-_{aq} in supercritical water (D_2O) at 400 °C, and most recently in H_2O at several different temperatures between 25 and 350 °C (see Section IV),[41] using picosecond time-resolved experiments in the range $\sim$60 ps to 6 ns.

Closer examination of the data presented in Fig. 5 shows that the variation of τ_s with temperature can be well represented by the empirical functional equation

$$\tau_s = At^{-n}, \qquad (6)$$

where n is the slope of the straight line in the log–log plot of τ_s against temperature shown in the inset of Fig. 5. A fit of eqn (6) to the data using a least-squares method gives $n \approx 0.775 \pm 0.015$. In other words, our calculations predict that τ_s is roughly inversely proportional to the temperature power 3/4 over the 25–350 °C temperature range studied.

Before closing, it is worth saying a few additional words on the (stoichiometric) relationship that exists between $G(Fe^{3+})$ and the various primary radical and molecular yields of the radiolysis of a deaerated aqueous 0.4 M H_2SO_4 solution [see eqn (1)]. In fact, to better assess the relative importance of these yields in the production of Fe^{3+} ions in the Fricke dosimeter, we present in Fig. 6 the results of our Monte-Carlo simulations showing the variations of the g-values for $H^\bullet$ (considering the conversion of e^-_{aq} to $H^\bullet$ in the spurs in acidic solution),[18] $^\bullet OH$, H_2O_2, H_2, and $HO_2^\bullet$ (calculated at the end of spur expansion, *i.e.*, at τ_s) as a function of temperature over the range 25–350 °C. As in neutral water[6,41] it is seen that, with

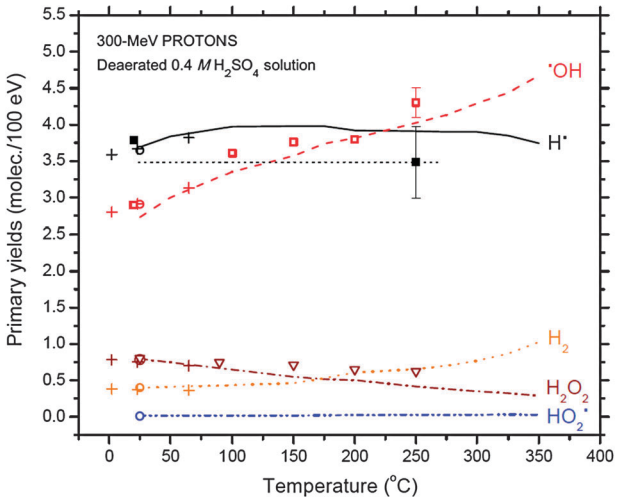

Fig. 6 Variations of the primary free-radical and molecular yields (in molec./100 eV), calculated at the end of spur expansion (*i.e.*, at τ_s) (see Fig. 5), of the radiolysis of deaerated 0.4 M H_2SO_4 aqueous solutions as a function of temperature over the range 25–350 °C. The different lines represent the results of our Monte-Carlo simulations performed with 300 MeV incident protons (LET ≈ 0.3 keV μm^{-1} at 25 °C) for $g(H^\bullet)$ (solid line), $g(^\bullet OH)$ (dashed line), $g(H_2O_2)$ (dash-dot line), $g(H_2)$ (dotted line), and $g(HO_2^\bullet)$ (dash-dot-dot line) (see text). Note that our simulations incorporate reaction (5) with a rate constant of 10^4 M^{-1} s^{-1} at 300 °C (ref. 59). Note also that the yield indicated "H•" in the figure actually represent the sum "e^-_{aq} + H•". Experimental data: (○) (ref. 1), (+) (ref. 44), (□, ■, ---) (ref. 51), and (▽) (ref. 62).

the exception of $g(H_2)$, the primary yields of free-radical products increase with increasing temperature while the molecular yield $g(H_2O_2)$ decreases. This general trend of having yields of free radicals that increase with temperature is explained from the fact that most important radical recombination reactions in the spur are *not* diffusion-controlled and therefore have rate constants that increase *less* with temperature than do the diffusion of the individual species out of the spur.[11,33,63] In other words, as the temperature increases, diffusion of the radical species out of spurs increases more rapidly than recombination, and one should anticipate less molecular recombination product. As one can see from Fig. 6, our computed results generally agree very well with experimental yields reported in the literature.[1,44,51,62,64] They are also in good accord with recent diffusion-kinetic model calculations in irradiated acidic water (data not shown here).[65] Of particular note is the remarkable agreement found between our calculated *g*-values for •OH and H• and those measured by Katsumura *et al.*[51] up to 250 °C. For example, these authors concluded that $g(H^\bullet)$ "seems to maintain an almost constant value" over their investigated range of temperatures. Such a result is very well reproduced by our calculations, which show that, indeed, $g(H^\bullet)$ varies little between 25 and 350 °C. Turning to the effect of temperature on the Fricke yield shown in Fig. 2 and 3, one can now better understand (or rather visualize), in light of the results shown in Fig. 6, why $G(Fe^{3+})$ increases with increasing temperature up to ~100–150 °C and why it is relatively temperature independent at higher temperatures. Clearly, $G(Fe^{3+})$ is highly sensitive to the primary *free-radical* yields, especially H• atoms (*via* formation of $HO_2^\bullet$) and also, but to a lesser degree (in fact, by a factor of ~3), hydroxyl radicals. Below ~100–150 °C, the increase in $G(Fe^{3+})$ is due primarily to the combined action of $g(H^\bullet)$ and $g(^\bullet OH)$, which both increases the contribution of H_2O_2 to the oxidation of Fe^{2+} ions to Fe^{3+} being only relatively inefficient in this temperature range. On the contrary, at higher temperatures, the combined reductions of $g(H^\bullet)$ and $g(H_2O_2)$ more or less counterbalance the increase in $g(^\bullet OH)$ with the net result that the observed Fricke yield appears as relatively independent of temperature.

VI. Conclusion

In this work, we have presented a simple procedure, based on the well-established reaction mechanism of the Fricke dosimeter, to estimate the temperature dependence of the lifetime of the spur (τ_s) in the low-LET radiolysis of water under ordinary irradiation conditions. This procedure uses Monte-Carlo simulations of the radiolysis of the ferrous sulfate (Fricke) dosimeter and of deaerated 0.4 M H_2SO_4 aqueous solutions at different selected times during spur expansion. τ_s is found to vary approximately as t^{-n} with $n \approx 0.775 \pm 0.015$ over the range 25 to 350 °C, going from ~4.2×10^{-7} s at 25 °C to ~5.7×10^{-8} s at 350 °C. To our knowledge, this is the first time that such a quantitative assessment of the time required for the changeover from spur kinetics to homogeneous kinetics is performed in the low-LET radiolysis of water as a function of temperature up to 350 °C. Moreover, our calculated $G(Fe^{3+})$ values compare very well with the available experimental data and are also in good accord with those predicted theoretically by other authors. This good overall agreement between calculated and experimental yield values gives, in turn, good support to the validity and consistency of the assumptions employed in this study.

Acknowledgements

We thank Professor D. M. Bartels, Dr A. J. Elliot, Professor K. Ghandi, Dr H. E. Sims, and Professor I. M. Svishchev for very useful discussions and correspondence, and for kindly sending us their experimental data prior to publication. One of us (Y. M.) wishes to thank the Japan Society for the Promotion of Science for its financial support dedicated to the present collaborative work. Particular thanks are also due to Dr D. A. Guzonas and Dr C. R. Stuart (Atomic Energy of Canada Limited, Chalk River Laboratories) for their continued help, support, and encouragement. The financial assistance provided by the Atomic Energy of Canada Limited, the Natural Sciences and Engineering Research Council of Canada, and the Natural Resources Canada through Canada's Generation IV National Program is gratefully acknowledged.

References

1 J. W. T. Spinks and R. J. Woods, *An Introduction to Radiation Chemistry*, Wiley, New York, 3rd edn, 1990.
2 C. Ferradini and J.-P. Jay-Gerin, *Can. J. Chem.*, 1999, **77**, 1542.
3 G. V. Buxton, in *Radiation Chemistry: Principles and Applications*, ed. Farhataziz and M. A. J. Rodgers, VCH Publishers, New York, 1987, p. 321.

4 J. A. LaVerne, in *Charged Particle and Photon Interactions with Matter. Chemical, Physicochemical, and Biological Consequences with Applications*, ed. A. Mozumder and Y. Hatano, Marcel Dekker, New York, 2004, p. 403.
5 B. C. Garrett, D. A. Dixon and D. M. Camaioni, *et al.* (46 authors), *Chem. Rev.*, 2005, **105**, 355.
6 A. J. Elliot and D. M. Bartels, The reaction set, rate constants and *g*-values for the simulation of the radiolysis of light water over the range 20 °C to 350 °C based on information available in 2008, Report AECL No. 153-127160-450-001, Atomic Energy of Canada Limited, Chalk River, Ontario, Canada, 2009.
7 T. Tippayamontri, S. Sanguanmith, J. Meesungnoen, G. R. Sunaryo and J.-P. Jay-Gerin, *Recent Res. Devel. Physical Chem.*, 2009, **10**, 143.
8 J. L. Magee, *Annual Review of Nuclear Science*, 1953, **3**, 171.
9 G. R. Freeman, in *Proceedings of the Workshop on the Interface between Radiation Chemistry and Radiation Physics*, Report ANL-82-88, ed. M. A. Dillon, R. J. Hanrahan, R. Holroyd, Y.-K. Kim, M. C. Sauer, Jr. and L. H. Toburen, Argonne National Laboratory, Argonne, Illinois, 1983, p. 9.
10 Throughout this paper, radiation chemical yields are quoted in units of molecules per 100 eV (abbreviated as "molec./100 eV"), as *g*(X) for primary yields and *G*(X) for experimentally measured yields. For conversion into SI units (mol J^{-1}), 1 molec./100 eV ≈ 0.10364 μmol J^{-1} (see ref. 2).
11 M.-A. Hervé du Penhoat, T. Goulet, Y. Frongillo, M.-J. Fraser, Ph. Bernat and J.-P. Jay-Gerin, *J. Phys. Chem. A*, 2000, **104**, 11757.
12 J. Meesungnoen, J.-P. Jay-Gerin, A. Filali-Mouhim and S. Mankhetkorn, *Can. J. Chem.*, 2002, **80**, 767.
13 G. Baldacchino, V. de Waele, H. Monard, S. Sorgues, F. Gobert, J. P. Larbre, G. Vigneron, J. L. Marignier, S. Pommeret and M. Mostafavi, *Chem. Phys. Lett.*, 2006, **424**, 77.
14 Y. Muroya, M. Lin, V. de Waele, Y. Hatano, Y. Katsumura and M. Mostafavi, *J. Phys. Chem. Lett.*, 2010, **1**, 331; Y. Muroya, unpublished data, 2010.
15 H. Fricke and E. J. Hart, in *Radiation Dosimetry*, ed. F. H. Attix and W. C. Roesch, Academic Press, New York, 3rd edn, 1966, vol. II, p. 167.
16 H. Fricke and S. Morse, *Am. J. Roentgenol. Radium Ther.*, 1927, **18**, 430; H. Fricke and S. Morse, *Philos. Mag.*, 1929, **7**, 129.
17 R. W. Matthews, *Int. J. Appl. Radiat. Isot.*, 1982, **33**, 1159.
18 At the acid concentration of 0.4 M H_2SO_4, the H^+ ions very rapidly scavenge most, if not all, of the e^-_{aq} radicals in spurs to form H• atoms (see, for example, C. Ferradini and J.-P. Jay-Gerin, *Res. Chem. Intermed.*, 2000, **26**, 549). In the presence of oxygen the H• atoms react with oxygen to form additional HO_2•.
19 A. O. Allen, *The Radiation Chemistry of Water and Aqueous Solutions*, D. Van Nostrand Co., Princeton, NJ, 1961.
20 R. C. Das, *Radiat. Res. Rev.*, 1971, **3**, 121.
21 N. Autsavapromporn, J. Meesungnoen, I. Plante and J.-P. Jay-Gerin, *Can. J. Chem.*, 2007, **85**, 214.
22 It should be stressed here that eqn (1) applies *only* if the radical and molecular yields intervening on the right-hand side of the equation are the "primary" yields, *i.e.*, those taken specifically at the time corresponding to the end of spur expansion τ_s.
23 J. Meesungnoen and J.-P. Jay-Gerin, *Radiat. Res.*, 2005, **164**, 688; J. Meesungnoen, M. Benrahmoune, A. Filali-Mouhim, S. Mankhetkorn and J.-P. Jay-Gerin, *Radiat. Res.*, 2001, **155**, 269.
24 S. M. Pimblott, M. J. Pilling and N. J. B. Green, *Radiat. Phys. Chem.*, 1991, **37**, 377.
25 S. M. Pimblott and N. J. B. Green, *Res. Chem. Kinet.*, 1995, **3**, 117.
26 Y. Frongillo, T. Goulet, M.-J. Fraser, V. Cobut, J. P. Patau and J.-P. Jay-Gerin, *Radiat. Phys. Chem.*, 1998, **51**, 245.
27 T. Goulet, M.-J. Fraser, Y. Frongillo and J.-P. Jay-Gerin, *Radiat. Phys. Chem.*, 1998, **51**, 85.
28 I. Plante, Développement de codes de simulation Monte-Carlo de la radiolyse de l'eau et de solutions aqueuses par des électrons, ions lourds, photons et neutrons: Application à divers sujets d'intérêt expérimental, *PhD thesis*, Université de Sherbrooke, 2009.
29 J. Meesungnoen and J.-P. Jay-Gerin, *J. Phys. Chem. A*, 2005, **109**, 6406; in *Charged Particle and Photon Interactions with Matter. Recent Advances, Applications, and Interfaces*, ed. Y. Hatano, Y. Katsumura and A. Mozumder, Taylor & Francis, Boca Raton, Florida, 2011, p. 355.
30 P.-Y. Jiang, Y. Katsumura, R. Nagaishi, M. Domae, K. Ishikawa, K. Ishigure and Y. Yoshida, *J. Chem. Soc., Faraday Trans.*, 1992, **88**, 1653.
31 Except for the peculiar bimolecular self-recombination of e^-_{aq} for which there is no evidence of any ionic strength effect (K. H. Schmidt and D. M. Bartels, *Chem. Phys.*, 1995, **190**, 145).
32 R. E. Weston, Jr. and H. A. Schwarz, *Chemical Kinetics*, Prentice-Hall, Englewood Cliffs, New Jersey, 1972. The function $f(I) = I^{1/2}/(1 + I^{1/2})$ that appears in eqn (2) is derived from the Debye–Hückel theory. It is known that this theory is limited to the low concentration regime and, more specifically, below about 0.1 M in concentration. Above this value of *I* the theory begins to show deviations. However, if one judges from Fig. 6.2 of the book of Weston and Schwarz, these deviations remain relatively limited even for the ion concentration range considered in Fricke solutions. There are other theories that work for higher ionic strengths, but they are based on experimentally determined coefficients that depend on types of ions present in the solution. There are no extensive tables of these coefficients, so their use is rather limited. Overall, the use of eqn (2) is a reasonable compromise especially as we have shown that taking into account the ionic strength in the rate constants actually had only little impact on the values of calculated yields.
33 A. J. Elliot, D. R. McCracken, G. V. Buxton and N. D. Wood, *J. Chem. Soc., Faraday Trans.*, 1990, **86**, 1539.
34 T. Solomon, *J. Chem. Educ.*, 2001, **78**, 1691.
35 In fact, in 0.4 M H_2SO_4, only ~3.5% of the total energy expended in the solution is initially taken up by HSO_4^- ions rather than by H_2O (assuming that the energy absorbed by each component is proportional to its electron fraction).
36 For solutions of 0.4 M in H_2SO_4 there is a small amount of •OH radicals that react with HSO_4^- to form the sulfate radical $SO_4^{\bullet -}$ according to $^\bullet OH + HSO_4^- \rightarrow H_2O + SO_4^{\bullet -}$ ($k = 1.5 \times 10^5$ M^{-1} s^{-1}) (see, for example, ref. 21, 23 and 30). However, the overall ferric ion yield remains the same as given by eqn (1) since the sulfate radical reacts with Fe^{2+} in the same way as $^\bullet OH$: $SO_4^{\bullet -} + Fe^{2+} \rightarrow Fe^{3+} + SO_4^{2-}$ ($k = 9.9 \times 10^8$ M^{-1} s^{-1}); see: P. Neta, R. E. Huie and A. B. Ross, *J. Phys. Chem. Ref. Data*, 1988, **17**, 1027, see also ref. 20.
37 T. Lundström, H. Christensen and K. Sehested, *Radiat. Phys. Chem.*, 2004, **69**, 211; H. Christensen, K. Sehested and T. Løgager, *Radiat. Phys. Chem.*, 1993, **41**, 575.
38 M. Běgusová and S. M. Pimblott, *Radiat. Prot. Dosim.*, 2002, **99**, 73.
39 J. P. Keene, *Radiat. Res.*, 1964, **22**, 14.
40 Note that thermal decomposition of H_2O_2 is not taken into account in the simulations. However, this process may not necessarily be negligible at temperatures above 150 °C; see, for example, A. J. Elliot, M. P. Chenier, D. C. Ouellette and V. T. Koslowsky, *J. Phys. Chem.*, 1996, **100**, 9014; J. Takagi and K. Ishigure, *Nucl. Sci. Eng.*, 1985, **89**, 177; see also ref. 6 and 38.
41 S. Sanguanmith, Y. Muroya, J. Meesungnoen, M. Lin, Y. Katsumura, L. Mirsaleh Kohan, D. A. Guzonas, C. R. Stuart and J.-P. Jay-Gerin, in *Proceedings of the 5th International Symposium on Supercritical Water-Cooled Reactors*, Vancouver, British Columbia, Canada, 13–16 March 2011, ISBN # 978-1-926773-02-5, Paper P091.
42 H. Christensen and K. Sehested, *J. Phys. Chem.*, 1986, **90**, 186; A. J. Elliot, Rate constants and *g*-values for the simulation of the radiolysis of light water over the range 0–300 °C, Report AECL-11073, Atomic Energy of Canada Limited, Chalk River, Ontario, Canada, 1994; T. W. Marin, K. Takahashi, C. D. Jonah, S. D. Chemerisov and D. M. Bartels, *J. Phys. Chem. A*, 2007, **111**, 11540.
43 Electrons in the subexcitation energy range (<7.3 eV in liquid water) are known to be very sensitive to the structural order of the surrounding medium, owing to their non-negligible delocalized character. See, for example, A. Mozumder, *Fundamentals of Radiation Chemistry*, Academic Press, San Diego, CA, 1999; T. Goulet and J.-P. Jay-Gerin, *Radiat. Res.*, 1989, **118**, 46; T. Goulet, J.-P. Jay-Gerin, Y. Frongillo, V. Cobut and M.-J. Fraser, *J. Chim. Phys.*, 1996, **93**, 111.
44 C. J. Hochanadel and J. A. Ghormley, *Radiat. Res.*, 1962, **16**, 653. These authors also reached a similar conclusion, pointing out that, at higher temperature, "subexcitation electrons are thermalized more rapidly".

45 D. Swiatla-Wojcik and G. V. Buxton, *J. Phys. Chem.*, 1995, **99**, 11464.
46 G. G. Jayson, B. J. Parsons and A. J. Swallow, *J. Chem. Soc., Faraday Trans. 1*, 1973, **69**, 236.
47 H. Christensen and K. Sehested, *Radiat. Phys. Chem.*, 1981, **18**, 723.
48 *CRC Handbook of Chemistry and Physics*, ed. W. M. Haynes, CRC Press, Boca Raton, Florida, 91st edn, 2010, p. 5–75.
49 P. J. Linstrom and W. G. Mallard (ed.), *NIST Chemistry Webbook*, NIST Standard Reference Database No. 69, National Institute of Standards and Technology, Gaithersburg, MD, 2005 (available at the http://webbook.nist.gov website).
50 Since the density of (pressurized) water decreases with increasing temperature (see ref. 49), this influences somewhat the particle's LET (the energy depositions become further apart when the temperature increases). For example, for 300 MeV irradiating protons, our computed average LET value at 350 °C is $\sim$0.19 keV μm^{-1}. This decrease in the LET with increasing temperature, however, has no particular effect on the Fricke yield values, which are known to remain nearly constant for LETs lower than $\sim$0.3 keV μm^{-1}. See, for example, N. V. Klassen, K. R. Shortt, J. Seuntjens and C. K. Ross, *Phys. Med. Biol.*, 1999, **44**, 1609; see also ref. 21.
51 Y. Katsumura, Y. Takeuchi and K. Ishigure, *Radiat. Phys. Chem.*, 1988, **32**, 259.
52 S. A. Kabakchi and I. E. Lebedeva, *High Energy Chem.*, 1984, **18**, 166.
53 I. Balakrishnan and M. P. Reddy, *J. Phys. Chem.*, 1972, **76**, 1273.
54 K. Ishigure, J. Takagi and H. Shiraishi, *Radiat. Phys. Chem.*, 1987, **29**, 195.
55 This value compares well with that ($\sim$0.85% per degree) predicted by Běgusová and Pimblott (ref. 38) from their stochastic IRT simulations of the γ-radiolysis of the aerated Fricke solution over this same 25–150 °C temperature range (see Fig. 2).
56 D. Swiatla-Wojcik and G. V. Buxton, *Radiat. Phys. Chem.*, 2005, **74**, 210.
57 D. M. Bartels, *Radiat. Phys. Chem.*, 2009, **78**, 191.
58 D. Swiatla-Wojcik and G. V. Buxton, *Radiat. Phys. Chem.*, 2010, **79**, 52.
59 K. Ghandi, C. D. Alcorn, G. Legate, P. W. Percival and J.-C. Brodovitch, in *Proceedings of the 2nd Canada-China Joint Workshop on Supercritical Water-Cooled Reactors*, Toronto, Ontario, 25–28 April 2010, ISBN # 0-919784-98-4; K. Ghandi, personal communication, 2010.
60 Homogeneity means that there are no statistical fluctuations in the number densities for all very small regions of the volume being examined. See, for example, G. A. Kenney and D. C. Walker, *J. Chem. Phys.*, 1969, **50**, 4074.
61 A preliminary report of these results is presented in D. A. Guzonas, C. R. Stuart, J.-P. Jay-Gerin, and J. Meesungnoen, Testing requirements for SCWR radiolysis, Report AECL No. 153-127160-REPT-001, Atomic Energy of Canada Limited, Chalk River, Ontario, Canada, 2010.
62 S. A. Kabakchi and I. E. Lebedeva, *High Energy Chem.*, 1987, **21**, 261.
63 A. J. Elliot, M. P. Chenier and D. C. Ouellette, *J. Chem. Soc., Faraday Trans.*, 1993, **89**, 1193.
64 A. J. Elliot, D. C. Ouellette, D. Reid and D. R. McCracken, *Radiat. Phys. Chem.*, 1989, **34**, 747.
65 D. Swiatla-Wojcik, *Nukleonika*, 2008, **53**(suppl. 1), S31.

